PHYSICAL REVIEW A VOLUME 22, NUMBER 6 DECEMBER 1980

Systematics of atom-atom collision strengths at high speeds

George H. Gillespie
Physical Dynamics, Inc., P.O. Box 1883, La Jolla, California 92038

Mitio Inokuti
Argonne National Laboratory, Argonne, Illinois 60439

(Received 30 May 1980)

The collision strengths for atom-atom collisions at high speeds are calculated in the first Born approximation. We studied four classes of collisions, distinguished depending upon whether each of the collision partners becomes excited or not. The results of numerical calculations of the collision strengths are presented for all neutral atoms with $Z \leq 18$. The calculations are based on atomic form factors and incoherent scattering functions found in the literature. The relative contribution of each class of collision processes to the total collision cross section is examined in detail. In general, inelastic processes dominate for low-Z atoms, while elastic scattering is more important for large Z. Other systematics of the collision strengths are comprehensively discussed. The relevant experimental literature has been surveyed and the results of this work for the three collision systems H-He, He-He, and H-Ar are compared with the data for electron-loss processes. Finally, suggestions are made for future work in measurements of atom-atom and ion-atom collision cross sections.

I. INTRODUCTION

When two complex atomic particles collide at a high relative speed there are a large variety of processes that can take place. For collisions involving two hydrogen atoms, Bates and Griffing[1] initiated a study of the various processes within the first Born approximation. Many other processes have been examined in subsequent work based largely on their formalism, as reviewed by Bell and Kingston.[2] In general, however, only the simpler atomic systems have been treated in detail, and little effort has been devoted to elucidating broad systematic features of atom-atom cross sections. We report here an initial undertaking toward that goal. It follows up several other recent studies[3-6] that have been devoted in part to the establishment of systematics of the relative importance of various phenomena relevant to fast ion-atom collisions.

Because there are a large number of possible final states which need to be addressed, it is useful to separate the processes into a few broad categories. For example, in the simpler case of electron-atom collisions, the various processes may be classified according to the transitions of the target atom alone, and the separation into elastic and total inelastic collisions provides a convenient partition.[7] For collisions involving two complex atomic particles the diversity of the possible processes increases correspondingly. In this paper we use a simple classification of the atomic processes according to whether either of the collision partners becomes excited or not. We thus consider four general classes of atom-atom cross sections and our approach is similar in spirit to other recent work primarily devoted to ion-atom collisions.[3,4,8] In the Born approximation at sufficiently high speeds, each of these cross sections σ behave asymptotically as v^{-2}, where v is the relative speed. The collision strengths, which are the same as $v^2\sigma$ to within a numerical factor, are thus constants and provide a compact means of comparing the relative importance of the various processes.

Section II provides the general theory for the cross sections and describes the numerical calculations. A concise tabulation of the collision strengths is included there. A comprehensive discussion of the systematics of the collision strengths is presented in Sec. III. Several examples are examined in detail and some results are compared with relevant experimental data. The question of the anticipated domain of validity of the collision strengths calculated in this work is treated in that section as well. Finally in Sec. IV we present some concluding remarks and offer some suggestions for future work in measurements of atom-atom or ion-atom collision cross sections.

II. THEORY AND NUMERICAL CALCULATIONS

A. General theory

Let us consider a collision of two neutral atoms A and B initially in their ground (electronic) states. The total energy of the Coulomb interactions between A and B is written as

$$V = Z_A Z_B e^2 R^{-1} - Z_A e^2 \sum_{k=1}^{Z_B} |\vec{R} + \vec{r}_k|^{-1} - Z_B e^2 \sum_{j=1}^{Z_A} |\vec{R} - \vec{r}_j|^{-1} + e^2 \sum_{j=1}^{Z_A} \sum_{k=1}^{Z_B} |\vec{r}_k - \vec{r}_j + \vec{R}|^{-1}, \tag{1}$$

where $\vec{R}$ is the distance from the A nucleus to the B nucleus, $\vec{r}_j$ is the position of the jth electron relative to the A nucleus, and $\vec{r}_k$ is the position of the kth electron relative to the B nucleus. By use of the Fourier integral, we may write V as

$$V = (2\pi^2)^{-1} e^2 \int d\vec{q} q^2 \left(Z_A Z_B \exp(-i\vec{q}\cdot\vec{R}) - Z_A \sum_{k=1}^{Z_B} \exp[-i\vec{q}\cdot(\vec{R}+\vec{r}_k)] - Z_B \sum_{j=1}^{Z_A} \exp[-i\vec{q}\cdot(\vec{R}-\vec{r}_j)] + \sum_{j=1}^{Z_A} \sum_{k=1}^{Z_B} \exp[-i\vec{q}\cdot(\vec{r}_k - \vec{r}_j + \vec{R})] \right). \tag{2}$$

In this representation, each term in V may be regarded as a product of functions of the form $\exp(i\vec{q}\cdot\vec{r}_j)$, $\exp(i\vec{q}\cdot\vec{r}_k)$, or $\exp(\pm i\vec{q}\cdot\vec{R})$.

Suppose that, after the collision, A emerges in state m and B in state n, where m or n may represent the ground state or any of the excited states, either discrete or continuum. We assume further that the relative speed v of the colliding partners is sufficiently great so that the first-order perturbation theory (i.e., the first Born approximation) is applicable. The domain of validity of this treatment depends upon the nature of m and n as well as upon the species A and B. We defer full discussion about the validity to Sec. III F. Within the first Born approximation, the cross section σ_{mn} for the collision

$$A + B \rightarrow A_m + B_n, \tag{3}$$

is expressed in terms of the matrix element of V taken between combined atomic states. By virtue of the product property of Eq. (2) noted earlier, the matrix element takes a product form. Specifically, the differential cross section $d\sigma_{mn}$ is given as

$$d\sigma_{mn} = 4\pi a_0^2 (v_0/v)^2 |F_m(K)|^2 |F_n(K)|^2 d(Ka_0)^2/(Ka_0)^4, \tag{4}$$

where $a_0 = \hbar^2/m_e e^2 = 0.529 \times 10^{-8}$ cm and $v_0 = \hbar/e^2 = c/137 = 2.188 \times 10^8$ cm/sec. The factor $(v_0/v)^2$ may be expressed as

$$(v_0/v)^2 = \mathrm{Ry}/T, \tag{5}$$

in terms of the Rydberg energy $\mathrm{Ry} = m_e e^4/2\hbar^2 = 13.6$ eV and of the symbol $T = \frac{1}{2} m_e v^2$, m_e being the *electron mass* used in Ref. 7. Further, $\hbar\vec{K}$ represents the momentum transfer in the collision, and its magnitude is given by

$$(Ka_0)^2 = 2(M/m_e)(T/\mathrm{Ry}) \times [1 - m_e E/2MT - (1 - m_e E/MT)^{1/2} \cos\theta], \tag{6}$$

where M is the *reduced mass* of the colliding partners, θ is the scattering angle measured in the center-of-mass frame, and E is the *sum* of electronic excitation energies E_m and E_n in A and B, respectively.

Most importantly, $F_m(K)$ is the matrix element between states of atom A:

$$F_m(K) = \left\langle m \left| Z_A - \sum_{j=1}^{Z_A} \exp(i\vec{K}\cdot\vec{r}_j) \right| 0 \right\rangle, \tag{7}$$

which we shall call the form factors. Similarly,

$$F_n(K) = \left\langle n \left| Z_B - \sum_{k=1}^{Z_B} \exp(i\vec{K}\cdot\vec{r}_k) \right| 0 \right\rangle. \tag{8}$$

Notice that $F_m(K)$ is a property of A only and $F_n(K)$ is a property of B only. To keep track of this distinction, we stipulate throughout that suffixes m and j always refer to atom A, and suffices n and k to atom B.

We also note that $F_{m=0}(K)$ is the Fourier transform of the charge density of atom A. For this case in which the final state is the same as the initial state, the *elastic* form factors are simply related to the well-known atomic form factor $F(K)$, e.g.,

$$F_{m=0}(K) = Z_A - F(K)_A. \tag{9}$$

For brevity of presentation, the present discussion will be restricted to nonrelativistic speeds $v \ll c$. Extension to mildly relativistic speeds is entirely straightforward and is virtually an exercise in kinematics, as it is so in the Bethe theory for structureless charged particles.[7] At extremely relativistic speeds, radiative effects such as coupling with bremsstrahlung will become appreciable and the Fermi density effect will be nonnegligible.

It is possible to integrate Eq. (4) formally over all possible values for $(Ka_0)^2$ (or alternatively, over all scattering angles θ) and thus to derive a compact formula for the integrated cross section σ_{mn} for high v. For this purpose, it is important to note the behavior of the form factor at small K. The familiar Taylor expansion leads to

$$F_0(K) = \tfrac{1}{2}(Ka_0)^2\langle X^2\rangle_0 - \tfrac{1}{24}(Ka_0)^4\langle X^4\rangle_0 + \cdots \quad (10)$$

for neutral atoms, and

$$F_{m\neq 0}(K) = -i(Ka_0)\langle X\rangle_m + (Ka_0)^2\langle X^2\rangle_m + \tfrac{1}{6}i(Ka_0)^3\langle X^3\rangle_m - \tfrac{1}{24}(Ka_0)^4\langle X^4\rangle_m + \cdots , \quad (11)$$

where

$$\langle X^\lambda\rangle_m = \left\langle m\left|\left(\sum_j X_j^\lambda\right)\right|0\right\rangle , \quad (12)$$

with

$$X_j = (\vec{K}\cdot\vec{r}_j)/Ka_0 . \quad (13)$$

Similar equations hold for $F_n(K)$ as well.

The meaning of the labels m and n for the electronic states of the atoms requires further clarification. In what follows, we assume that the atoms in the initial states are either spherical or randomly oriented. We also imply by the label m or n that the customary summation over magnetic quantum numbers of the atomic final state is to be taken. In summary we assume rotational symmetry for the states designated by m or n. Under this stipulation, the squared absolute value of each form factor is an even function of the *scalar variable* K. We have tacitly used the stipulation already when we write Eq. (4), in which only scalar K appears.

We now distinguish four classes of collisions: (1) elastic collisions, i.e., $m=0$ and $n=0$, (2) singly inelastic collisions, i.e., $m=0$ and $n\neq 0$, (3) singly inelastic collisions of another kind, i.e., $m\neq 0$ and $n=0$, (4) doubly inelastic collisions, i.e., $m\neq 0$ and $n\neq 0$. Let us treat each class in some detail.

Elastic collisions [class (1)]

The total collision cross section is given as

$$\sigma_{00} = 4\pi a_0^2\frac{\mathrm{Ry}}{T}\int_0^{(K_{\max}a_0)^2} |F_{m=0}(K)|^2 \times |F_{n=0}(K)|^2\frac{d(Ka_0)^2}{(Ka_0)^4} . \quad (14)$$

The lower limit of the integration is zero for elastic collisions. The upper limit is given by

$$(K_{\max}a_0)^2 = 4(M/m_e)^2(T/\mathrm{Ry}) , \quad (15)$$

which is a large number because $M/m_e \gg 1$. The integrand is analytic for $(Ka_0)^2 \geq 0$. Thus, we may write the integral as

$$\int_0^\infty - \int_{(K_{\max}a_0)^2}^\infty .$$

The first contribution is obviously independent of T. The second contribution is approximately $-\tfrac{1}{4}Z_A^2Z_B^2(m_e/M)^2(\mathrm{Ry}/T)$, because at large K the form factor behaves as Z_A or Z_B. We define the collision strength as

$$I_{\mathrm{el},\mathrm{el}}(A,B) \equiv I_{00}(A,B) = (T/\mathrm{Ry})(\sigma_{00}/8\pi a_0^2) , \quad (16)$$

and obtain to a good approximation at high speeds

$$I_{\mathrm{el},\mathrm{el}}(A,B) = \int_0^\infty |F_{m=0}(K)|^2|F_{n=0}(K)|^2\frac{d(Ka_0)}{(Ka_0)^3} . \quad (17)$$

Singly inelastic collisions [classes (2) and (3)]

Let us discuss the case in which $m\neq 0$ and $n=0$. The total cross section is given as

$$\sigma_{m0} = 4\pi a_0^2\frac{\mathrm{Ry}}{T}\int_{(K_{\min}a_0)^2}^{(K_{\max}a_0)^2} |F_m(K)|^2|F_{n=0}(K)|^2\frac{d(Ka_0)^2}{(Ka_0)^4} . \quad (18)$$

The lower limit of the integration is now nonvanishing, it has the value

$$(K_{\min}a_0)^2 = (E_m^2/4\,\mathrm{Ry}\,T)[1 + \tfrac{1}{2}(m_eE_m/MT) + O(m_eE_m/MT)^2] , \quad (19)$$

i.e., exactly the same as the value for inelastic collisions of A with a structureless particle [Eq. (2.17) of Inokuti[7]]. Similarly, the upper limit is given by

$$(K_{\max}a_0)^2 = 4(T/\mathrm{Ry})(M/m_e)^2 \times [1 - \tfrac{1}{2}(m_eE_m/MT) + O((m_eE_m/MT)^2)] . \quad (20)$$

From Eqs. (10) and (11), we immediately find that the integrand is analytic for $K\geq 0$. Generally $(K_{\min}a_0)^2$ is a small number (see, however, the second paper under Ref. 4) and $(K_{\max}a_0)^2$ is a large number. The integral may be written as

$$\int_0^\infty - \int_0^{(K_{\min}a_0)^2} - \int_{(K_{\max}a_0)^2}^\infty .$$

The first contribution is independent of T and is dominant. The second contribution may be estimated by use of Eqs. (10) and (11); it roughly amounts to

$$\int_0^{(K_{\min}a_0)^2} \simeq \tfrac{1}{8}|\langle X\rangle_m|^2|\langle X^2\rangle_0|^2(K_{\min}a_0)^2 \simeq \tfrac{1}{32}|\langle X\rangle_m|^2|\langle X^2\rangle_0|^2E_m^2/\mathrm{Ry}\,T . \quad (21)$$

To estimate the third contribution, one recalls the high-K behavior of the form factors

$$|F_m(K)|^2 = O((Ka_0)^{-8}) , \quad (22)$$

$$|F_{n=0}(K)|^2 = Z_B + O((Ka_0)^{-4}) , \quad (23)$$

as given by Rau and Fano.[9] Therefore the third

contribution is only $O((K_{\max}a_0)^{-5})$ and utterly negligible.

Consequently, we write the collision strength

$$I_{m0}(A,B) = (T/\mathrm{Ry})(\sigma_{m0}/8\pi a_0^2) = \int_0^\infty |F_m(K)^2|F_{n=0}(K)|^2 \frac{d(Ka_0)}{(Ka_0)^3}. \quad (24)$$

Notice that the quantity $|F_{n=0}(K)|^2$ here plays the role of an effective charge on atom B, which causes excitation of atom A. At small values of Ka_0 (which corresponds to large impact parameters), the effective charge is negligibly small because of the screening of atomic electrons in B. For this reason, the collision strength lacks a $\ln T$ term, which is familiar in the collision strength for excitation by charged structureless particles. Indeed, when B is an ion of either charge having an electronic structure, a $\ln T$ term arises and ultimately at high T dominates the collision strength, as seen in Refs. 3 and 4.

The sum of σ_{m0} over all $m \neq 0$ may be called the total cross section $\sigma_{\mathrm{in,el}}$ for collisions of class (2). The method of Inokuti, Kim, and Platzman[10] may be readily extended[3,4] to the evaluation of $\sigma_{\mathrm{in,el}}$. The basis of this method is the sum rule

$$\sum_{m\neq 0} |F_m(K)|^2 = \left\langle \left| \sum_{j=1}^{Z_A} \exp(i\vec{K}\cdot\vec{r}_j) \right|^2 \right\rangle - \left| \left\langle \sum_{j=1}^{Z_A} \exp(i\vec{K}\cdot\vec{r}_j) \right\rangle \right|^2, \quad (25)$$

obtained by the well-known closure relation, where $\langle\,\rangle$ denotes a ground-state expectation value. The entity on the right-hand side of Eq. (25) is well known in x-ray physics; it corresponds to the quantity $Z_A S_{\mathrm{inc},A}(K)$, i.e., Z_A multiplied by the incoherent scattering function of atom A.

The summation of $\sigma_{m0}(A,B)$ is straightforward by use of Eq. (25). We have

$$I_{\mathrm{in,el}}(A,B) = (T/\mathrm{Ry})(\sigma_{\mathrm{in,el}}/8\pi a_0^2) = \int_0^\infty Z_A S_{\mathrm{inc},A}(K)|F_{n=0}(K)|^2 \frac{d(Ka_0)}{(Ka_0)^3}. \quad (26)$$

The case in which $m=0$ and $n\neq 0$ requires no new treatment; one obtains all results by interchanging m and n in the above treatment.

Doubly inelastic collisions [class (4)]

For this last case, the cross section for a fixed set of labels m and n is given as

$$\sigma_{mn} = 4\pi a_0^2 \left(\frac{\mathrm{Ry}}{T}\right) \int_{(K_{\min}a_0)^2}^{(K_{\max}a_0)^2} |F_m(K)|^2 |F_n(K)|^2 \frac{d(Ka_0)^2}{(Ka_0)^4}. \quad (27)$$

the limits of the integrations are

$$(K_{\min}a_0)^2 = [(E_m+E_n)^2/4\,\mathrm{Ry}\,T] \times [1 + \tfrac{1}{2}m_e(E_m+E_n)/MT + O((m_e(E_m+E_n)/MT)^2)] \quad (28)$$

and

$$(K_{\max}a_0)^2 = 4(T/\mathrm{Ry})(M/m_e)[1 + O(m_e(E_m+E_n)/MT)]. \quad (29)$$

Because of Eq. (11), both form factors behave as Ka_0 for small Ka_0, and therefore the integrand is analytic for $(Ka_0)^2 \geq 0$.

Analysis along the same lines as for singly inelastic collision leads to

$$\sigma_{mn} = 4\pi a_0^2 \left(\frac{\mathrm{Ry}}{T}\right)\left(\int_0^\infty |F_m(K)|^2 |F_n(K)|^2 \frac{d(Ka_0)^2}{(Ka_0)^4} \cdot + O((E_m+E_n)^2/\mathrm{Ry}\,T)\right). \quad (30)$$

The summation of σ_{mn} over all $m\neq 0$ and $n\neq 0$ proceeds as before. The result is expressed as $\sigma_{\mathrm{in,in}}$ and $I_{\mathrm{in,in}}(A,B)$, given by

$$I_{\mathrm{in,in}}(A,B) = (T/\mathrm{Ry})(\sigma_{\mathrm{in,in}}/8\pi a_0^2) = (T/\mathrm{Ry}) \sum_{m\neq 0}\sum_{n\neq 0} (\sigma_{m,n}/8\pi a_0^2) = \int_0^\infty Z_A S_{\mathrm{inc},A}(K) Z_B S_{\mathrm{inc},B}(K) \frac{d(Ka_0)}{(Ka_0)^3}. \quad (31)$$

The corrections to the right-most expression amount to $O(Z_A Z_B\,\mathrm{Ry}/T)$. A precise estimate is given in Refs. 3 and 4. It should also be mentioned that additional corrections to these asymptotic collision strengths can arise from electron exchange, Bethe ridge effects,[4,7] as well as non-Born contributions to the cross sections (e.g., polarization or distortion).

The principal numerical task of this work is the evaluation of the momentum-transfer integrals given by Eqs. (17), (26), and (31). Notice that the integrands depend only on ground-state properties of the atoms: the incoherent scattering functions $S_{\mathrm{inc}}(K)$, and the atomic form factors $F(K)$ [via Eq. (9)]. These functions have been studied by many authors (see Ref. 11, for example). Since only ground-state wave functions are required, both $S_{\mathrm{inc}}(K)$ and $F(K)$ have been calculated with some precision for many atoms, and we can anticipate that the asymptotic collision strengths described in the next section will reflect this precision. Finally, remarks on collisions between two hydrogenic systems are given in Ref. 3, and a summary of that discussion is presented in the Appendix.

B. Numerical calculations

For the calculation of the collision strengths, we have used extensive tabulations of atomic form factors and incoherent scattering functions given by other workers, and it is necessary to include a few comments regarding our choice of tabulations. One goal of this work is to provide as accurate a set of collision strengths as possible. However, our primary aim was to examine the systematics of the collision strengths, which necessitates that results from one atom to the next be comparable on a relative basis. Because the level of sophistication of the ground-state wave functions utilized by others in their calculations of $F(K)$ and $S_{\rm inc}(K)$ generally decreases with increasing Z, these two aims are not always compatible and some compromises have been made. Generally we adopted as a starting point the tabluations given by Hubbell *et al.*,[11] and supplemented it with results based on more accurate atomic wave functions when available. Their results for all atoms are given on a common grid of momentum transfer, which aids in carrying out numerical integrations with high relative accuracy. For atoms lighter than nitrogen, that tabulation is based primarily on the work of Brown,[12] who used wave functions including configuration interactions. The remainder of that tabulation which we have used ($Z \leq 18$) is based primarily on the work of Cromer and Mann,[13] who used Hartree-Fock wave functions. Additional tables we used are the configuration-interaction results for C ^3P, N $^4S^0$, O ^3P, and Ne ^1S given by Tanaka and Sasaki,[14] and the results of Naon *et al.*,[15] for Ar.

In carrying out the numerical integrations in Eqs. (17), (26), and (31), we have fit the data at low momentum transfer [$(Ka_0) < 0.1$] according to the limiting forms

$$F_0(K) \simeq F_0'(0)(Ka_0)^2 , \tag{32}$$

$$ZS_{\rm inc}(K) \simeq M_{\rm tot}^2 (Ka_0)^2 . \tag{33}$$

Both coefficients appearing in Eqs. (32)–(33) may be calculated from ground-state expectation values:

$$F_0'(0) = \tfrac{1}{2}\langle X^2 \rangle = \tfrac{1}{6}\left\langle \sum_I \vec{r}_I^{\,2} \right\rangle , \tag{34}$$

$$M_{\rm tot}^2 = \tfrac{1}{3}\left\langle \left(\sum_I \vec{r}_I \right)^2 \right\rangle . \tag{35}$$

Inokuti *et al.*[16] have given a comprehensive summary of results for $M_{\rm tot}^2$, and values of $F_0'(0)$ for Hartree-Fock wave functions may be obtained from Fischer's tabulation of $\langle \vec{r}_I^{\,2} \rangle$ values.[17] Our calculations used values for these parameters which were estimated directly from the tabulated form factors and incoherent scattering functions according to Eqs. (32) and (33). For completeness we give these adopted values in Table I, together with appropriate results from other sources.[16,17] There are several differences between comparable cases which may be noted, particularly for Na, Mg, and Al. However, these discrepancies have only a small impact on our collision strength calculations. For example, the largest differences in both $M_{\rm tot}^2$ and $F_0'(0)$ are for Na, where the discrepancies are about 3%. However, the Na-Na collision strengths $I_{\rm el,el}$ and $I_{\rm el,in}$ are unchanged, while $I_{\rm in,in}$ is increased by less than 0.4% if the larger values of $M_{\rm tot}^2$ and $F_0'(0)$ are utilized in the low momentum transfer region. Since the numerical integrations have an absolute accuracy of about 1%, improvements in these parameters will have a negligible effect on our results.

C. Summary of numerical results

In Table II we summarize the results for the elastic ($I_{\rm el,el}$) and doubly inelastic ($I_{\rm in,in}$) collision strengths based on the tabulations of Hubbell *et al.*[11] Because of the symmetry of $I_{\rm el,el}$ (or $I_{\rm in,in}$) under the interchange of collision partners, only an upper (or lower) triangular matrix is required in order to specify all possibilities. Table II is a superposition of such an upper triangular matrix for values of $I_{\rm el,el}$, and a lower triangular matrix for values of $I_{\rm in,in}$. For example, for the fully elastic collision process

$$\mathrm{C}(g) + \mathrm{Ne}(g) \rightarrow \mathrm{C}(g) + \mathrm{Ne}(g) ,$$

one obtains $I_{\rm el,el} = 113$ (from row 6 and column 10). For the doubly inelastic collision

$$\mathrm{C}(g) + \mathrm{Ne}(g) \rightarrow \mathrm{C}(\Sigma) + \mathrm{Ne}(\Sigma) ,$$

one gets $I_{\rm in,in} = 8.25$ (from row 10 and column 6). Similarly for collisions between identical atoms the upper diagonal gives $I_{\rm el,el}$ and the lower diagonal $I_{\rm in,in}$.

Table III gives the corresponding results for the singly inelastic collision strengths ($I_{\rm el,in}$). In Table III the ordered pair subscript notation is chosen such that atoms labeled vertically correspond to the first subscript on the collision strength, while the horizontal labels are to be associated with the second subscript. For example, the collision strength $I_{\rm el,in}$ for the process

$$\mathrm{C}(g) + \mathrm{Ne}(g) \rightarrow \mathrm{C}(g) + \mathrm{Ne}(\Sigma) ,$$

(from the 6th row and 10th column of Table III) is 22.7. On the other hand, for the process in which the Ne atom remains in the ground state, but the C is either collisionally excited or ionized, i.e.,

$$\mathrm{Ne}(g) + \mathrm{C}(g) \rightarrow \mathrm{Ne}(g) + \mathrm{C}(\Sigma) ,$$

TABLE I. Adopted values of M^2_{tot} and $F_0'(0)$ for the low-Ka_0 behavior of $F_0(K)$ and $S_{inc}(K)$ based on the tabulations of Hubbell *et al.*[a] For comparison, M^2_{tot} results from Inokuti *et al.*[b] and values of $F_0'(0)$ determined from Fischer's[c] data are also given.

Atom	Z	M^2_{tot} (Adopted)[a]	M^2_{tot} (Inokuti)[b]	$F_0'(0)$ (Adopted)[a]	$F_0'(0)$ (Fischer)[c]
H	1	1	1	0.5	0.5
He	2	0.7525	0.7525	0.402	0.3978
Li	3	6.00	6.037 (CI)	3.06	3.105 (HF)
Be	4	3.96	4.046 (CI)	2.71	2.886 (HF)
B	5	3.52	3.544 (CI)	2.59	2.642 (HF)
C	6	2.94	2.953 (CI)	2.30	2.299 (HF)
N	7	2.92	2.947 (HF)	2.08	2.014 (HF)
O	8	2.53	2.550 (HF)	1.87	1.861 (HF)
F	9	2.25	2.257 (HF)	1.70	1.706 (HF)
Ne	10	2.02	2.024 (HF)	1.56	1.562 (HF)
Na	11	7.97	8.206 (HF)	4.39	4.256 (HF)
Mg	12	8.99	9.190 (HF)	4.87	4.935 (HF)
Al	13	8.74	8.896 (HF)	5.49	5.579 (HF)
Si	14	7.91	8.036 (HF)	5.39	5.377 (HF)
P	15	7.17	7.227 (HF)	5.12	5.046 (HF)
S	16	6.51	6.543 (HF)	4.84	4.860 (HF)
Cl	17	5.90	5.966 (HF)	4.59	4.605 (HF)
Ar	18	5.42	5.477 (HF)	4.31	4.339 (HF)

[a] Based on low-Ka_0 tabulations of Ref. 11.

[b] From Table I of Ref. 16: CI values for Li through C, HF values for N through Ar.

[c] These are obtained by using $F_0'(0) = \frac{1}{6}\sum_{i=1}^{Z} \langle 0|\vec{r}_i^2|0\rangle$, with $\vec{r}_i^2$ values from H, analytic, He-Ar, Ref. 17.

the collision strength is 29.5 (from the 10th row and 6th column).

Finally in this section we include Tables IV and V, which give a subset of collision strengths for the atoms $Z=6-10$ and 18, based on atomic form factors and incoherent scattering functions of Tanaka and Sasaki,[14] and Naon *et al.*[15] Since the wave functions used by these authors include correlation effects, these collision strengths provide a basis upon which to examine the accuracy of the results in Tables II and III for $Z \geq 7$, which are based on Hartree-Fock wave functions. The importance of configuration interactions in accurately describing the incoherent scattering function of atoms (~20% at low K) has been pointed out by various authors.[11-15] Likewise, the relative insensitivity (<5%) of the atomic form factor to such effects has been discussed frequently.[11-15] We anticipate then that the doubly inelastic collision strengths will display the largest variations in going from HF to CI wave functions (decreasing in general), with $I_{el,\,in}$ and $I_{el,\,el}$ showing increasingly smaller variations. A quick comparison of the collision strengths in Tables II–V verifies this expectation; we shall discuss these differences in more detail in later sections.

As indicated previously, the accuracy of the numerical integrations carried out for the results presented in this section is about 1%. It is primarily associated with the size of the momentum transfer grid and the corresponding interpolations which are required. However, the relative accuracy of two collision strengths calculated from atomic data on the same grid is considerably higher. For example, the collision strengths $I_{in,\,in}$ for oxygen and flourine colliding with sulfur (from Table II) are 17.1 and 17.0. This trend is a real effect and the percentage different given by these numbers is probably a reliable estimate of the size of this change. On the other hand, comparison between results obtained from different tabulations must be made with some care.

III. SYSTEMATICS OF THE COLLISION STRENGTHS

A large amount of information is embodied in the data given in Tables II–V. Our goal in this work regarding systematic features of these results is twofold. First, we shall examine the most significant, broad features of each of the collision strengths individually (Secs. III A–III C), as well as comparatively (Sec. III D). Second, by way of example, we discuss in Sec. III D some of the more detailed results which may be gleaned from the tables and, in Sec. III E, some of the applications for which the results may be utilized. Section III F concludes with a discussion of the anticipated region of validity of our collision strengths.

TABLE II. Elastic collision strengths $I_{el,el}$, and doubly inelastic collision strengths $I_{in,in}$ for all atom-atom collisions with $Z \leq 18$. The upper right triangular matrix gives values for $I_{el,el}$, and the lower left triangular matrix gives the values of $I_{in,in}$; see Sec. II C. of the text for further discussion. The collision strengths in this table are based on the atomic form factors and incoherent scattering functions tabulated by Hubbell *et al.* (Ref. 11).

	1	2	3	4	5	6	7	8	9	10	11	12	13	14	15	16	17	18	
1	0.634	0.118	0.261	0.641	1.24	1.95	2.65	3.31	3.89	4.41	4.88	5.71	6.79	8.04	9.44	10.9	12.4	13.8	15.3	H
2	0.718	0.892	0.679	1.45	2.68	4.27	6.03	7.84	9.62	11.3	13.0	15.0	17.4	20.2	23.3	26.7	30.2	34.0	37.8	He
3	1.75	1.86	5.58	4.03	7.41	11.1	14.7	18.1	21.4	24.5	27.5	33.4	40.3	48.1	56.0	63.8	71.5	79.1	86.5	Li
4	2.00	2.23	5.80	6.46	14.2	21.5	28.3	34.6	40.2	45.4	50.3	60.8	73.8	88.5	104	119	134	149	163	Be
5	2.18	2.51	6.04	6.91	7.53	33.2	44.4	54.7	64.0	72.4	80.0	95.2	114	137	161	185	210	233	256	B
6	2.19	2.61	5.88	6.87	7.60	7.77	60.3	75.5	89.3	102	113	133	158	187	219	253	287	321	354	C
7	2.37	2.87	6.30	7.43	8.25	8.49	9.29	95.7	115	132	148	173	203	238	278	320	364	408	452	N
8	2.34	2.90	6.10	7.28	8.17	8.49	9.33	9.44	139	162	183	212	247	289	335	385	437	491	546	O
9	2.28	2.90	5.90	7.10	8.03	8.42	9.28	9.45	9.51	190	217	251	291	338	391	448	508	571	636	F
10	2.21	2.86	5.68	6.87	7.82	8.25	9.12	9.33	9.44	9.42	249	288	334	386	444	508	577	648	722	Ne
11	3.16	3.71	9.33	10.2	11.1	11.2	12.2	12.1	12.0	11.8	17.2	337	394	457	527	601	679	760	844	Na
12	3.80	4.34	11.3	12.4	13.3	13.3	14.4	14.2	14.0	13.7	20.3	24.3	463	540	624	712	803	897	992	Mg
13	4.14	4.74	12.1	13.4	14.4	14.5	15.7	15.5	15.3	14.9	21.8	26.2	28.2	634	734	839	945	1050	1160	Al
14	4.31	4.99	12.3	13.8	15.0	15.1	16.4	16.3	16.1	15.7	22.5	26.9	29.2	30.2	853	976	1100	1230	1350	Si
15	4.34	5.10	12.1	13.8	15.1	15.4	16.7	16.7	16.5	16.2	22.6	27.0	29.2	30.4	30.7	1120	1260	1410	1550	P
16	4.41	5.25	12.1	14.0	15.4	15.7	17.1	17.1	17.0	16.7	22.9	27.2	29.6	30.8	31.2	31.9	1430	1600	1760	S
17	4.42	5.34	11.9	13.9	15.4	15.8	17.4	17.4	17.4	17.1	23.0	27.2	29.6	31.0	31.5	32.2	32.6	1790	1970	Cl
18	4.37	5.35	11.7	13.7	15.3	15.8	17.3	17.5	17.5	17.2	22.9	26.9	29.3	30.7	31.3	32.1	32.5	32.5	2190	Ar
	H	He	Li	Be	B	C	N	O	F	Ne	Na	Mg	Al	Si	P	S	Cl	Ar		

TABLE III. Singly inelastic collision strengths $I_{el,in}$ for all atom-atom collisions with $Z \leq 18$. The atoms labeled vertically are scattered elastically (el) while those labeled horizontally are scattered inelastically (in); see Sec. II C. of the text for further discussion. The collision strengths in this table are based on the atomic form factors and incoherent scattering functions tabulated by Hubbell *et al.* (Ref. 11).

	1	2	3	4	5	6	7	8	9	10	11	12	13	14	15	16	17	18	
1	0.207	0.297	0.468	0.617	0.741	0.817	0.917	0.964	0.995	1.01	1.12	1.26	1.38	1.48	1.56	1.64	1.70	1.74	H
2	0.371	0.597	0.874	1.14	1.40	1.60	1.81	1.97	2.09	2.17	2.35	2.55	2.76	2.95	3.13	3.30	3.47	3.60	He
3	1.37	1.80	3.42	4.28	4.90	5.18	5.74	5.90	6.00	6.02	7.36	8.55	9.37	9.93	10.2	10.6	10.9	11.0	Li
4	2.55	3.40	5.96	7.73	9.02	9.67	10.7	11.1	11.3	11.3	13.3	15.3	16.8	18.0	18.7	19.5	20.1	20.4	Be
5	3.69	5.11	8.45	11.1	13.2	14.3	16.0	16.6	17.1	17.2	19.6	22.2	24.5	26.3	27.5	28.8	29.8	30.4	B
6	4.59	6.63	10.4	13.8	16.5	18.3	20.5	21.6	22.4	22.7	25.3	28.3	31.0	33.3	35.0	36.9	38.4	39.3	C
7	5.32	7.99	12.2	16.0	19.4	21.7	24.5	26.1	27.2	27.8	30.6	33.8	36.9	39.7	41.8	44.1	46.1	47.5	N
8	5.89	9.15	13.6	17.9	21.8	24.7	27.9	30.0	31.6	32.5	35.4	38.8	42.1	45.2	47.8	50.5	52.8	54.6	O
9	6.36	10.2	14.9	19.5	23.9	27.2	30.9	33.4	35.4	36.7	39.8	43.3	46.8	50.2	53.1	56.2	58.9	61.1	F
10	6.74	11.0	16.0	21.0	25.7	29.5	33.5	36.5	38.9	40.5	43.8	47.4	51.2	54.8	58.0	61.3	64.4	66.9	Ne
11	8.72	13.5	21.2	27.3	32.8	36.8	41.6	44.7	47.2	48.9	54.5	60.1	65.1	69.4	73.0	76.7	80.0	82.6	Na
12	11.0	16.5	26.6	34.4	41.0	45.5	51.2	54.5	57.2	58.9	66.4	74.0	80.5	85.9	90.0	94.4	98.2	101	Mg
13	13.7	19.9	32.7	42.3	50.2	55.4	62.2	65.9	68.7	70.4	79.9	89.6	97.7	104	109	114	119	122	Al
14	16.1	23.5	38.1	49.7	59.1	65.2	73.2	77.4	80.5	82.5	93.3	105	114	122	128	134	140	143	Si
15	18.4	26.9	43.0	56.4	67.4	74.6	83.8	88.8	92.4	94.5	106	119	130	139	146	153	159	164	P
16	20.4	30.3	47.5	62.5	75.1	83.4	93.9	99.7	104	106	119	132	144	155	163	171	178	183	S
17	22.3	33.5	51.7	68.0	82.1	91.7	103	110	115	118	131	145	158	170	179	188	196	202	Cl
18	23.9	36.5	55.5	73.1	88.6	99.5	112	120	126	129	142	157	171	184	194	204	214	220	Ar
	H	He	Li	Be	B	C	N	O	F	Ne	Na	Mg	Al	Si	P	S	Cl	Ar	

TABLE IV. Elastic collision strengths $I_{el,el}$, and doubly inelastic collision strengths $I_{in,in}$, for all atom-atom collisions with $6 \leq Z \leq 10$, or $Z = 18$. The upper right triangular matrix gives values for $I_{el,el}$, and the lower left triangular matrix gives the values of $I_{in,in}$; see Sec. II C. of the text for further discussion. The collision strengths in this table are based on the atomic form factors and incoherent scattering functions tabulated by Tanaka and Sasaki (Ref. 14) and for C through Ne, and by Naon *et al.* (Ref. 15) for Ar.

	6	7	8	9	10	18	
6	7.82	60.1	74.8	89.1	101	113	351	C
7	7.78	7.81	94.5	114	131	148	446	N
8	7.92	8.01	8.25	139	161	183	542	O
9	7.89	8.03	8.31	8.40	189	217	631	F
10	7.74	7.92	8.24	8.36	8.36	250	719	Ne
18	13.9	14.1	14.6	14.7	14.6	2160	25.9	Ar
	C	N	O	F	Ne	Ar		

A. Elastic collisions, $I_{el,el}$

Among the four classes of collision strengths which we have considered in this work, the total elastic collision strength displays the largest absolute variation with the atomic numbers of the collision partners. Figure 1 shows a plot of $I_{el,el}$ from Table II versus Z_A and Z_B. As is evident from that figure, the elastic collision strength is a monotonically and sharply increasing function of the atomic numbers of the collision partners. While this increase is definitely monotonic, there are discernible undulations in the surface of $I_{el,el}$. In particular, troughs in the elastic collision strength surface are clearly evident where one of the collision partners is either He or Ne. This is, of course, a reflection of the closed shells of these atoms.

In general, we anticipate that the total elastic collision strengths will have a rough dependence

TABLE V. Singly inelastic collision strengths $I_{el,in}$ all atom-atom collisions with $6 \leq Z \leq 10$ or $Z = 18$. The atoms labeled vertically are scattered elastically (el) while those labeled horizontally are scattered inelastically (in); see Sec. II C. of the text for further discussion. The collision strengths in this table are based on the atomic form factors and incoherent scattering functions tabulated by Tanaka and Sasaki (Ref. 14) for C through Ne, and by Naon *et al.* (Ref. 15) for Ar.

	6	7	8	9	10	18	
6	18.3	19.3	20.5	21.1	21.4	36.4	C
7	21.5	23.0	24.7	25.6	26.2	44.1	N
8	24.7	26.7	28.7	30.1	30.9	51.6	O
9	27.2	29.6	32.1	33.9	35.0	58.1	F
10	29.5	32.4	35.4	37.5	38.9	64.3	Ne
18	98.4	106	114	119	122	205	Ar
	C	N	O	F	Ne	Ar	

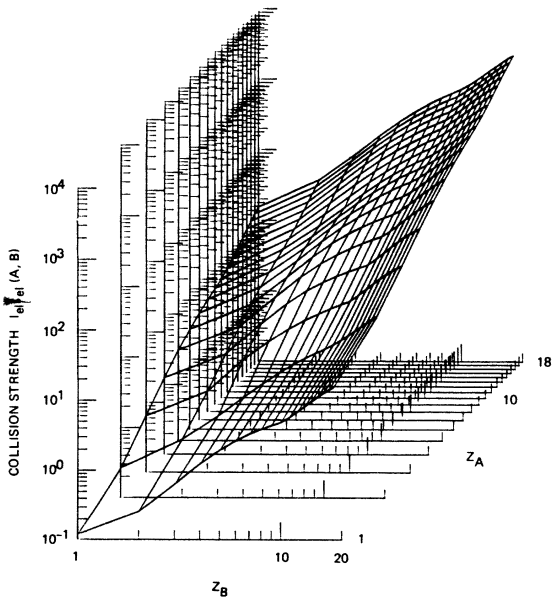

FIG. 1. Plot of the fully elastic collision strengths $I_{el,el}(A,B)$ as a function of the atomic numbers of the collision partners Z_A and Z_B. These collision strengths are from Table II and are based on the atomic form factors tabulated by Hubbell *et al.* (Ref. 11). The elastic collision strengths increase rapidly with atomic number, scaling roughly as $Z_A^2 Z_B^2$ according to Eq. (36). Slight undulations in the surface reflect the effects of shell structure.

on Z_A and Z_B of the form

$$I_{\mathrm{el,el}}(A,B)=\mathcal{I}_{\mathrm{el,el}}Z_A^2Z_B^2. \tag{36}$$

This scaling with respect to the square of the atomic numbers is simply a reflection of the dominance of the (screened) internuclear Coulomb interaction. The factor $\mathcal{I}_{\mathrm{el,el}}$ may be considered a reduced collision strength, and presumably should display a much reduced dependence on Z_A and Z_B throughout the periodic table. In a global sense we expect it to be roughly constant, independent of the atomic numbers. However, we would also anticipate that $\mathcal{I}_{\mathrm{el,el}}$, when plotted as a function of Z_A and Z_B, to more clearly display the effects of shell structure since the gross scaling of (36) has been removed. Figure 2 shows a plot of the reduced collision strength. The surface is indeed relatively flat (note the significant change in the logarithmic vertical scales from Fig. 1), with well defined minima along lines associated with closed shells. Maxima at H and B, and to a lesser extent near P, indicate that these atoms are relatively large from the point of view of elastic collisions. As a final comment in this section, we note that the scaling given in Eq. (36) is valid to within a factor of 5 for all the elastic collisions considered in this work, with a constant reduced collision strength[18] $\mathcal{I}_{\mathrm{el,el}}=2.2\times10^{-2}$.

B. Singly inelastic collisions, $I_{\mathrm{el,in}}$ and $I_{\mathrm{in,el}}$

The singly inelastic collision strengths from Table III are plotted in Fig. 3, again as a function of the atomic numbers. A monotonically increasing dependence on both Z_A and Z_B is apparent, but the trends are not equally steep in both directions. Undulations of this collision strength surface are also again clear, only slightly more pronounced than for elastic collisions, the troughs again being associated with closed shells.

For this collision strength we anticipate the scaling with the atomic numbers Z_A and Z_B is described roughly by

$$I_{\mathrm{el,in}}(A,B)=\mathcal{I}_{\mathrm{el,in}}Z_A^2Z_B. \tag{37}$$

For the elastically scattered particle (A), the scaling again reflects the strong coherent effect of the nuclear Coulomb potential. The inelastically scattered particle (B) has a scaling linear in

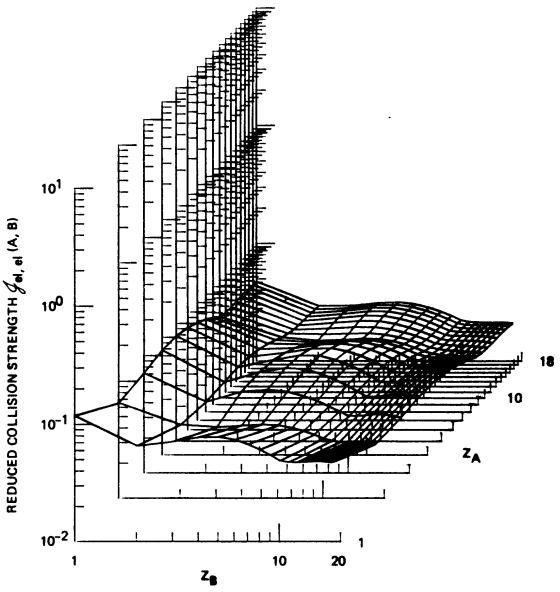

FIG. 2. Reduced elastic collision strength $\mathcal{I}_{\mathrm{el,el}}(A,B)$ as a function of the atomic numbers of the collision partners, Z_A and Z_B. The gross scaling [Eq. (36)] of the elastic collision strengths in Fig. 1 has been removed and the general flatness of the surface reflects the accuracy of that approximation. (Note the significant change of vertical scale from Fig. 1.) Minima in the surface at He, Ne, and Ar reflect the "smallness" of those closed-shell atoms.

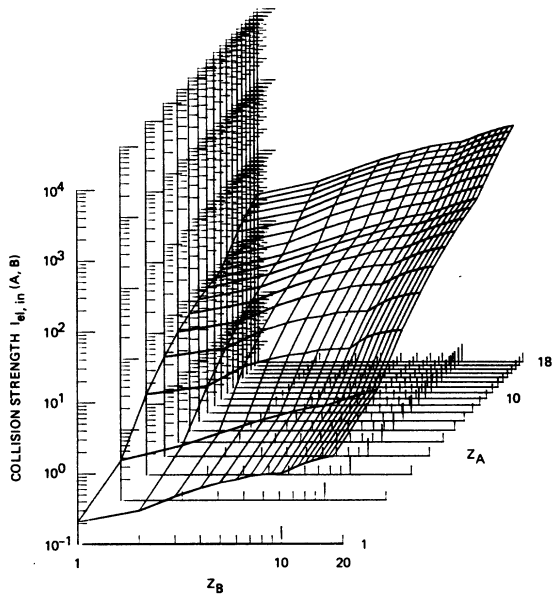

FIG. 3. Plot of the singly inelastic collision strength $I_{\mathrm{el,in}}(A,B)$ as a function of the atomic numbers of the collision partners, Z_A and Z_B. These collision strengths are from Table III and are based on the atomic form factors (particle A) and incoherent scattering functions (particle B) tabulated by Hubbell *et al.* (Ref. 11). The singly inelastic collision strengths increase monotonically with atomic numbers, scaling roughly as $Z_A^2Z_B$ as given by Eq. (37). Undulations in the surface are again a reflection of shell structure. The singly inelastic collision strengths $I_{\mathrm{in,el}}$ may be obtained by symmetry $I_{\mathrm{in,el}}(A,B)=I_{\mathrm{el,in}}(B,A)$.

the atomic number. This scaling arises from the number of electrons in the atom, and reflects the incoherent sum of all possible electronic transitions in the atom. Again, we may regard $g_{el,in}$ as a reduced collision strength and in Fig. 4 we display this reduced collision strength as a function of the atomic numbers. The relative flatness of this surface attests to the general validity of the scaling (37), although the variations in the $g_{el,in}$ surface associated with shell effects are somewhat more apparent than for $g_{el,el}$. Ridges and valleys of relative maxima and minima are essentially the same as for the reduced elastic collision strength, and all-in-all, Figs. 2 and 4 are qualitatively quite similar. For the singly inelastic collision strengths the scaling of Eq. (37) provides a reasonable description of the gross features for $g_{el,in} = 4.2 \times 10^{-2}$, again reproducing all of the exact results to within a factor of 5.[18]

C. Doubly inelastic collisions, $I_{in,in}$

The doubly inelastic collision strengths show the effects of shell structure most dramatically of the four classes of collision strengths we have considered. Figure 5 displays $I_{in,in}$ from Table II in the same format as utilized in Figs. 1 and 3. Shell-structure effects are so pronounced in this case that the collision strength is no longer monotonically increasing. A valley of local minima is present whenever either of the collision partners is Ne, and local minima also occur when one collision partner is Ar. However, the collisions of O-Ar, F-Ar, and somewhat surprisingly He-Ar and Ne-Ar are an exception; these collision strengths being somewhat larger than those for O-Cl, F-Cl, He-Cl, and Ne-Cl. These "exceptions" represent exceedingly small numerical deviations, and while we believe this accurately reflects the situation for the case of Hartree-Fock models of Cl and Ar, the actual case may well be somewhat different. All of the collision strengths displayed in Fig. 5 for either Z_A or $Z_B \geq 7$ will shift downward significantly (several percent) if atomic models more accurate than Hartree-Fock are used. This is readily apparent upon comparing Tables II and IV, for example. Nevertheless, the primary qualitative features of $I_{in,in}$ are unlikely to be modified by more accurate calculations, and

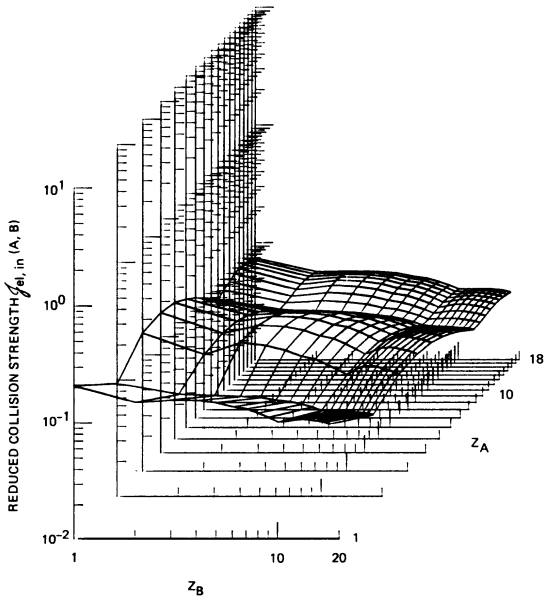

FIG. 4. Reduced singly inelastic collision strength $g_{el,in}(A,B)$ as a function of the atomic numbers of the collision partners, Z_A and Z_B. The gross scaling [Eq. (37)] of the singly inelastic collision strengths (in Fig. 3) has been removed, and the general flatness of the surface reflects the accuracy of that approximation. (Again the change in vertical scale from Fig. 3 to Fig. 4 should be noted.) Minima near the "small" closed-shell atoms of He, Ne, and Ar are again apparent.

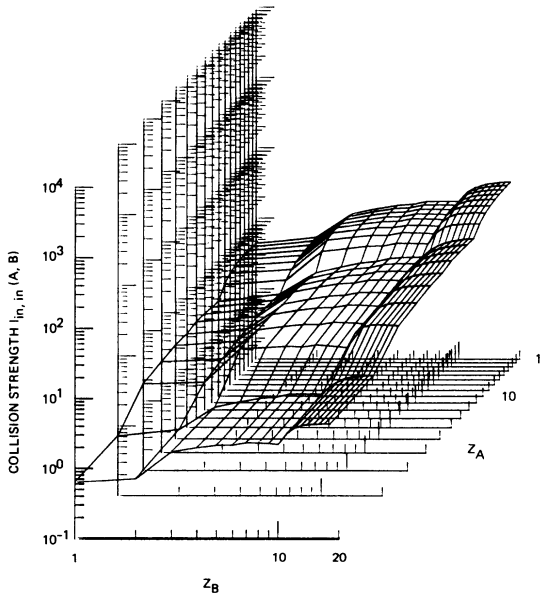

FIG. 5. Plot of the doubly inelastic collision strength $I_{in,in}(A,B)$ as a function of the atomic numbers of the collision partners, Z_A and Z_B. These collision strengths are also from Table II which are based on the incoherent scattering functions tabulated by Hubbell *et al.* (Ref. 11). The scaling of the doubly inelastic collision strength is roughly proportional to $Z_A Z_B$ as given by Eq. (38), but shell structure effects are pronounced and this collision strength does not increase monotonically with increasing atomic numbers.

the clearly larger significance of shell structure on this collision strength appears well established.

The doubly inelastic collision strength also has a relatively simple scaling for the gross trend with respect to increasing Z_A or Z_B, i.e.,

$$I_{\mathrm{in,in}}(A,B) = \mathcal{I}_{\mathrm{in,in}} Z_A Z_B \,. \tag{38}$$

The doubly inelastic reduced collision strength $\mathcal{I}_{\mathrm{in,in}}$ is shown in Fig. 6. As we would anticipate from the above discussion, this figure displays significantly larger undulations in the $\mathcal{I}_{\mathrm{in,in}}$ surface than the corresponding Figs. 2 and 4 for $\mathcal{I}_{\mathrm{el,el}}$ and $\mathcal{I}_{\mathrm{el,in}}$. However, the scaling (38) is again relatively accurate for describing the overall general trend with Z. For $\mathcal{I}_{\mathrm{in,in}} = 1.3 \times 10^{-1}$ all of the collision strengths $I_{\mathrm{in,in}}$ calculated in this work are reproduced by Eq. (38) to within a factor of 5.[18]

D. Comparisons among the four classes of collision strengths

As is apparent from the discussion in III A.–III C., each of the four classes of collision strengths considered in this work have significantly different general scaling laws as well as varying degrees of variation from these scaling rules due to shell structure. Clearly, when both Z_A and Z_B are large enough, elastic collisions will be dominant at very high energies. In the case of collisions between two hydrogen atoms, however, Bates and Griffing[1] already showed that doubly inelastic collisions were dominant. A natural question which emerges then is where are the boundaries in the Z_A-Z_B plane which delineate the different regions in which each of the collision strengths is dominant? We now answer this question. Figure 7 shows a plot of the domains in which each of the four classes of collision strengths considered here is largest. For any combination of collisions between H, He, or Li the doubly inelastic collision strength is the largest. For H colliding with any other atom, the singly inelastic collisions are dominant, with the H atom being either excited or ionized while the other collision partner remains in its ground state. This collision strength is also dominant for several cases in which He collides with atoms of atomic number greater than three. For most of the possible combinations of collision partners, including all of those with both Z_A and Z_B greater than three, the elastic collision strength is the largest.

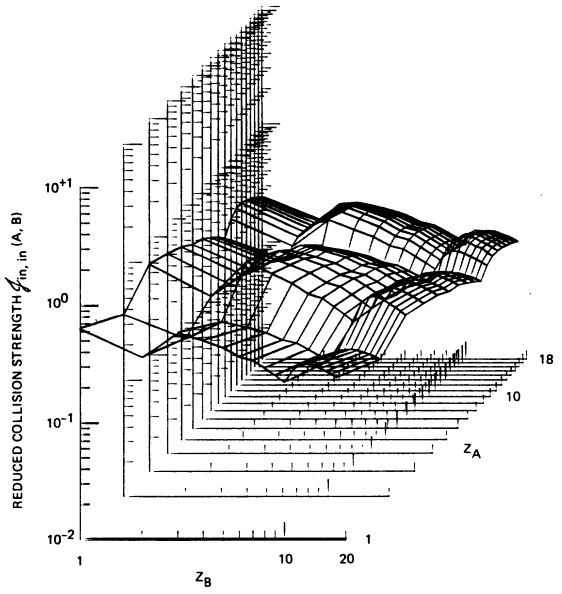

FIG. 6. Reduced doubly inelastic collision strength $\mathcal{I}_{\mathrm{in,in}}(A,B)$ as a function of the atomic numbers of the collision partners, Z_A and Z_B. The gross scaling [Eq. (38)] of the doubly inelastic collision strengths in Fig. 5 has been removed. The somewhat larger oscillations in the surface (as compared to Figs. 2 and 4) reflect the more pronounced effects of atomic shell structure on the doubly inelastic collision strength.

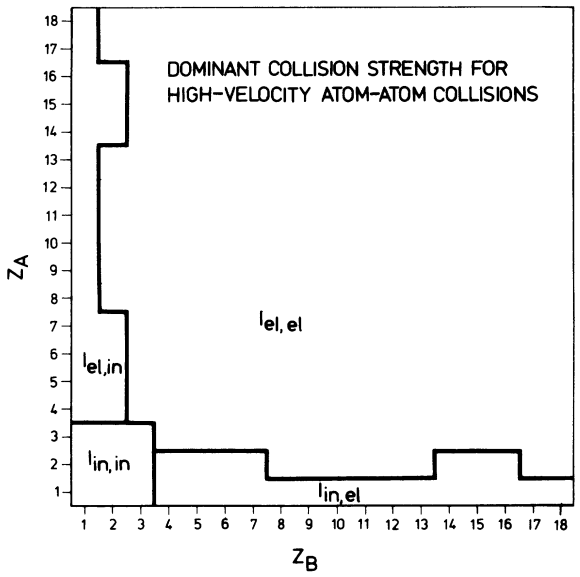

FIG. 7. Domains indicating the largest collision strength for the four classes of collisions considered in this work. The first subscript on each collision strength is associated with particle A, the second with particle B. For collisions between any two atoms with atomic numbers less than or equal to three, doubly inelastic collisions ($I_{\mathrm{in,in}}$) are dominant at very high energies. If one particle is hydrogen (and in select cases helium), then singly inelastic collisions ($I_{\mathrm{el,in}}$) are dominant if the other collision partner has an atomic number greater than three. For the vast majority of possible collision partners however, elastic collisions ($I_{\mathrm{el,el}}$) are dominant at very high energies.

One may also ask how Fig. 7 might be altered if elastic collisions were not considered, i.e., which of the remaining three inelastic collision strengths is dominant? A quick examination of the data in Tables II and III shows that the doubly inelastic domain is not enlarged; it is still only dominant for collisions involving H, He, and Li. Singly inelastic collisions then become dominant for all other cases, with the collision partner of lower Z being either excited or ionized, while that of the higher Z remains in its ground state following the collision.

In a rigorous sense we can only argue that the domains indicated in Fig. 7 will correctly indicate the largest cross section (for the four classes of collisions considered) at asymptotically high speeds. In particular, the asymptotic collision strengths given in Tables II and III can only be expected to give equally good results for all the cross sections if the speed is sufficiently high that our basic assumptions are satisfied in all cases. As indicated earlier and discussed more fully in Sec. III F., the velocities above which our collision strengths should give a quantitative description of the cross sections depends in each case upon Z_A and Z_B, as well as upon each of the four classes of collisions. At subasymptotic energies then, we anticipate that the boundaries in Fig. 7 will be altered somewhat, and at low energies they may be quite different. Where the cross sections are falling significantly with increasing velocity, though perhaps not as fast as v^{-2}, Fig. 7 should still provide a reasonable guide for estimating which class of collisions will have the dominant cross section.

To further examine the relative importance of the various collision processes considered, we now take a detailed look at the case of carbon colliding with other atoms. This example is chosen primarily because it also permits us to make some comparisons between Tables II and III and IV and V. Otherwise it is a fairly typical example and permits us to display some of the results more concretely via a case study.

Figure 8 displays the four collision strengths for carbon colliding with neutral atoms as a function of the target atom atomic number. Three of these curves are in essence cuts at $Z_A = 6$ through the surfaces displayed in Figs. 1, 3, and 5; the fourth collision strength ($I_{\text{in,el}}$) is obtained by symmetry from Fig. 3 (using a cut along $Z_B = 6$). The results shown as solid circles in Fig. 8 for target atoms with $Z_B < 7$, and as open circles for $Z_B \geq 7$, are from Tables II and III. As discussed in Secs. IIB. and IIC., these collision strengths are based on Hartree-Fock (HF) wave functions for $Z_B \geq 7$, and on more accurate wave functions that include configuration interactions (CI) for $Z_B \leq 6$. For comparison we also include additional results as solid circles for $7 \leq Z_B \leq 10$ and $Z_B = 18$ from Tables IV and V, all of which used CI wave functions. The differences in $I_{\text{el, in}}$ and $I_{\text{in, in}}$ between the curves formed from solid and open symbols thus displays the difference between CI and HF model wave functions for the target atom. This is a quantitative confirmation of the general expectation mentioned in Sec. IIC. that the difference in the incoherent

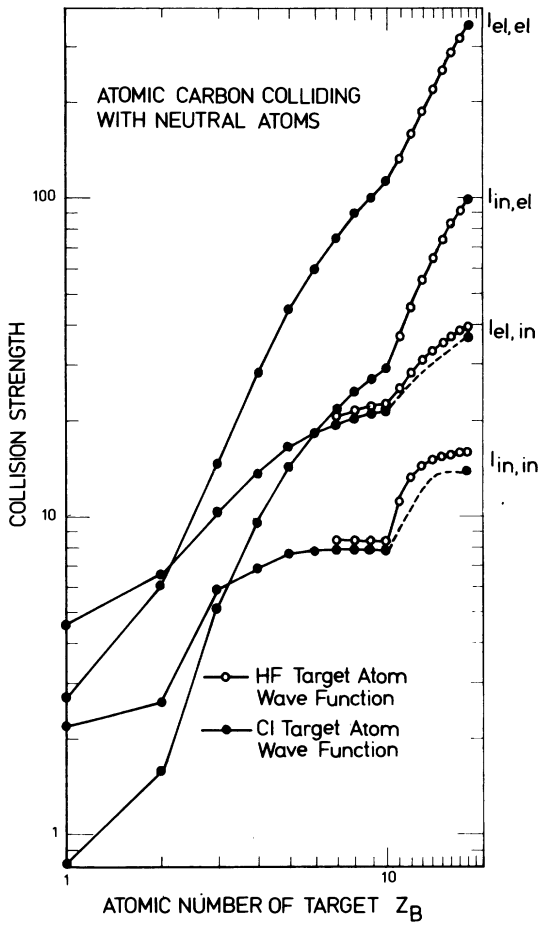

FIG. 8. The four collision strengths calculated for an incident carbon atom colliding with neutral target atoms, all plotted as a function of the atomic number Z_B of the target. The open circles are results for Hartree-Fock (HF) models of the atoms and are taken from the data in Tables II and III ($Z_B > 6$). The solid circles are results based on configuration-interaction (CI) atomic models. For $Z_B \leq 6$ these results are also from Tables II and III, but for $7 \leq Z_B \leq 10$ and $Z_B = 18$ they are taken from Tables IV and V. The solid lines are simply to aid the eye in following each of the collision strengths, the broken curves are only intended to suggest how $I_{\text{el, in}}$ and $I_{\text{in, in}}$ might look for $11 \leq Z_B \leq 17$ if CI wave functions for these atoms were to be used in the calculations.

scattering function for CI and HF wave functions may affect these collision strengths. On the other hand, the overlap of these symbols for $I_{el,el}$ and $I_{in,el}$ reiterates the lack of significant difference between different atomic models. In all cases we recommend results based on CI wave functions wherever available, although for many applications the results based on HF wave functions are probably adequate.

The scaling properties for the various collision strengths discussed in Secs. III A.–III C. are also reflected in Fig. 8: $I_{el,el}$ and $I_{in,el}$ have a rough proportionality to Z_B^2, while $I_{el,in}$ and $I_{in,in}$ increase more like Z_B. The more pronounced effects of shell structure on $I_{el,in}$ and $I_{in,in}$ are also apparent. The dominance of $I_{el,in}$ for $Z_B=1$ or 2, and of $I_{el,el}$ for $Z_B \geq 3$ (as displayed in Fig. 7), are put on a quantitative basis in Fig. 8 for this case of incident carbon atoms.

E. Comparisons with electron-loss cross section data

The inelastic collision strengths calculated in this work include transitions to all final states, either discrete bound states or final states in the continuum which most often lead to ionization. On general grounds[4] the asymptotic inelastic cross sections must be strongly dominated by final states in the continuum for atom-atom collisions. Experimentally, ionization cross sections at high speeds are also easier to measure than either elastic or discrete-state excitation cross sections. In order to compare some of our results with experimental data, we have thus restricted our examination to total electron-loss cross sections at high speeds. The results of a literature survey[19–24] for this data are summarized in Fig. 9, where we display as a function of Z_A and Z_B the availability of experimental data on the high-

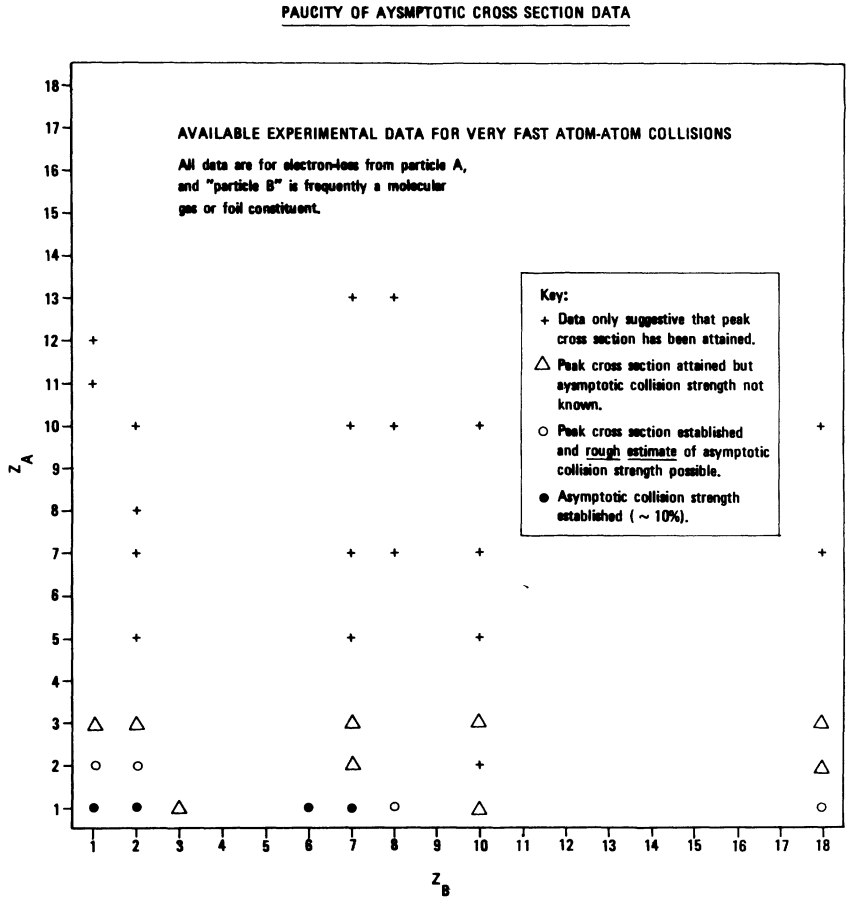

FIG. 9. Summary of the available data for electron-loss cross sections in fast atom-atom collisions. This summary is based upon data obtained from Dehmel *et al.* (Ref. 19: +, $Z_A>3$; △ and +, $Z_A=2$); Tawara and Russek (Ref. 20: ○ and △, $Z_A=1, Z_B=3$, 8, and 10); Pedersen and Hvelplund (Ref. 21: △, $Z_A=3$; Ref. 22: ○, $Z_A=2$); Acerbi *et al.* (Ref. 23: ●, $Z_A=1, Z_B=1$, 2, and 7; ○, $Z_A=1, Z_B=18$); and Webber and Hojvat (Ref. 24: ●, $Z_A=1, Z_B=6$).

energy electron-loss cross sections.

As a function of increasing kinetic energy of the incident atom, the electron-loss cross section first increases, reaches a maximum typically in the 10–100-keV/amu energy region, and then decreases, eventually falling as v^{-2} at sufficiently high velocity. It is in this asymptotic region that our collision strengths are rigorous, and we especially sought data extending into that regime. We have thus classified the experimental cross section data into four categories in Fig. 9: those for which the data is only suggestive that the maximum cross section has been reached, those for which the maximum seems to have been attained but little information on the asymptotic cross section can be extracted, those for which the maximum is well established and one can make a rough estimate of the asymptotic value, and those cases for which the asymptotic cross section is established. This latter group is clearly small. We have found only four examples, all of which involve a hydrogen atom as the projectile. Furthermore, in many cases the target atom is frequently one constituent of either a molecular gas or a foil, and consequently detailed comparisons must be made with some caution. In some instances the incident atomic beam may also have contained some metastable states, further complicating the matter.

Figure 10 shows the electron-loss collision strengths for H incident on He, a case for which the potential ambiguities cited above should not be a problem. The open symbols are collision strengths obtained from the experimental data[23,25–34] for $\sigma_{0,1}$ according to

$$I=(8\pi a_0^2\alpha^2/\beta^2)^{-1}\sigma_{0,1}$$
$$=\beta^2\sigma_{0,1}/(3.75\times10^{-20}\ \mathrm{cm}^2). \quad (39)$$

where $\beta=v/c$. The solid line is the asymptotic collision strength $I_{\mathrm{in,el}}+I_{\mathrm{in,in}}$ calculated in this work. The ionization collision strength ($I_{\mathrm{ion,el}}+I_{\mathrm{ion,in}}$) has been calculated previously for this case and those results are shown for comparison by the dashed line, and the dashed curve shows how that asymptotic collision strength is altered if the next-order term in the v^{-2} expansion is retained.[4] The experimental and theoretical asymptotes for the electron-loss collision strength are in very good agreement for $E_{\mathrm{lab}}\gtrsim1$ MeV. The inelastic collision strength $I_{\mathrm{in,el}}+I_{\mathrm{in,in}}$ of this work is about 18% above the ionization collision strength, the difference arising from the contribution of excitations to discrete bound states of the hydrogen projectile.

Figure 11 summarizes the electron-loss data[22,28,35–37] for He-He collisions. The peak cross section is well established and data extends to energies about one order-of-magnitude greater than that corresponding to the maximum cross section. The asymptotic collision strength may be roughly estimated to be 1.3 ~ 1.4. This estimate of the asymptotic collision strength for the total electron-loss process for He + He is consistent with our result $I_{\mathrm{in,el}}+I_{\mathrm{in,in}}=1.49$, shown by the solid line in Fig. 11. Following arguments similar to those of the last paper cited under Ref. 4, we anticipate that the ionization collision strength

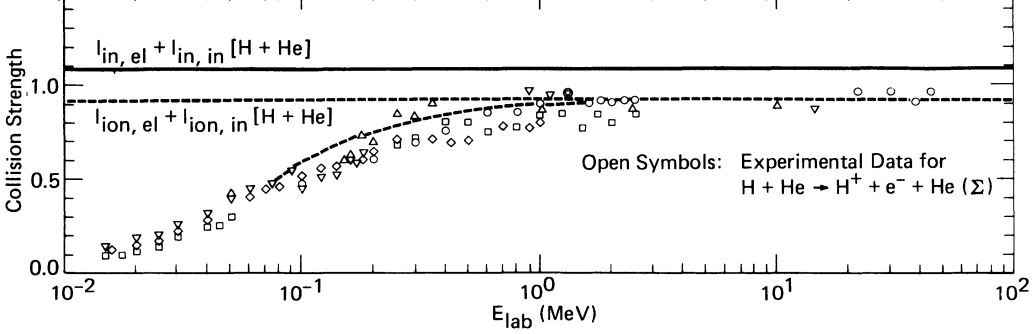

FIG. 10. Comparison of the theoretical asymptotic collision strength with experiment for H+ He. Symbols are $(8\pi a_0^2\alpha^2/\beta^2)^{-1}\sigma_{0,1}$ where $\sigma_{0,1}$ are the experimental cross sections for electron loss from atomic H colliding with He. Data are shown only for energies above that corresponding to the maximum experimental cross section (~15 keV), and are taken from: ▽ 0.05–0.18 MeV, Solov'ev *et al.* (Ref. 25); 0.9–1.3 MeV, Dimov and Dudnikov (Ref. 26); 14.6 MeV, Smythe and Toevs (Ref. 27); △ 0.15–0.4 MeV, Puckett *et al.* (Ref. 28); 1.0 and 2.4 MeV, Welsh *et al.* (Ref. 29); 10 MeV, Berkner *et al.* (Ref. 30); □ 0.05–2.5 MeV, Williams (Ref. 31); ◇ 0.05–0.2 MeV, Steir and Barnett (Ref. 32); 0.25–1 MeV, Barnett and Reynolds (Ref. 33); ○ 0.1–2.5 MeV, Toburen *et al.* (Ref. 34); 22–45 MeV, Acerbi *et al.* (Ref. 23). Solid line is the theoretical result of this work for $I_{\mathrm{in,el}}+I_{\mathrm{in,in}}$ which is a rigorous upper bound to the electron-loss collision strength. For comparison the theoretical electron-loss collision strength $I_{\mathrm{ion,el}}+I_{\mathrm{ion,in}}$ from Ref. 4 is given by the dashed line, and the dashed curve shows that collision strength including next-order (low-energy) corrections.

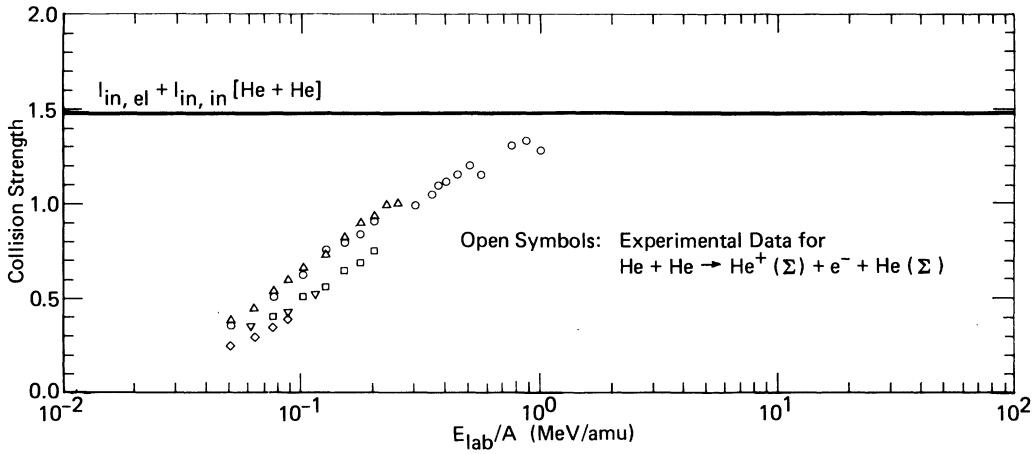

FIG. 11. Comparison of theoretical asymptotic collision strength with experiment for He+ He. Open symbols are $(8\pi a_0^2\alpha^2/\beta^2)^{-1}(\sigma_{0,1}+\sigma_{0,2})$, where $\sigma_{0,1}$ and $\sigma_{0,2}$ are the single and double electron-loss cross sections, except for that from Ref. 28 which is $\sigma_{0,1}+2\sigma_{0,2}$. (However, $\sigma_{0,2} \ll \sigma_{0,1}$, so this is a minor difference.) Data are shown only for energies above that corresponding to the maximum experimental cross section (~50 keV/amu) and are taken from: ○ Pederson and Hvelplund (Ref. 22); △ Puckett *et al.* (Ref. 28); ▽ Allison (Ref. 35); □ Pivovar *et al.* (Ref. 36); and ◇ Gilbody *et al.* (Ref. 37). Solid line is the theoretical result of this work for $I_{in,el}+I_{in,in}$ which is a rigorous upper bound to the total electron-loss collision strength. It is also expected to be a reasonably good approximation (≲20%) to the asymptotic electron-loss collision strength.

should lie closer to the inelastic collision strength for He + He collisions (as compared to the 18% difference for H + He collisions) since $M_{ion}^2/M_{tot}^2 = 0.650$ for He (as compared to 0.283 for H). Although theory and experiment are consistent, a definitive conclusion is not yet possible. A quantitative comparison must await data at higher energies, although we should point out that only modestly higher energy is required; 2 MeV/amu or so appears adequate.

Figure 12 gives results for the heavier target atom Ar, again with H as the projectile. Extensive data are available for the cross section for electron loss from the H projectile at energies above that corresponding to the maximum cross section. Even at 45 MeV/amu however, the collision strength has still apparently not quite reached an asymptotic value. We can estimate the asymptotic collision strength as 2.3 ~ 2.5, but again higher energy data (~100 MeV) appears necessary to establish the value conclusively. The inelastic collision strengths we calculated for both HF and CI Ar wave functions (solid and dash-dot lines) are shown and lie 10–25% above the estimates of the experimental asymptote for electron loss. The previously calculated[4] electron-loss collision strength $I_{ion,el}+I_{ion,in}$ is also shown (dashed line), including the low-energy correction (dashed curved). The experimental and theoretical asymptotes for electron loss are thus consistent, but in contrast to the case of H + He collisions, the low-energy correction does not give an adequate description of the departure from the asymptote. This is a limitation of the applicability of the full Born approximation to heavy-particle scattering.[39] It is tempting to suggest that the region of validity of the Born approximation in this case is the same as the region of validity of the asymptote alone. Further data will be required to establish this region experimentally, however.

As a final remark in this section we should point out that the plots of collision strength versus the logarithm of the kinetic energy/amu, as shown in Figs. 10–12, are a generalization of Fano plots.[7,40] There is an important difference in the appearance of the plots in the asymptotic region, however, when compared to inelastic collisions of structureless charged particles. For atom-atom collisions the collision strengths approach constant values because of the absence of any long-range Coulomb potential, whereas the traditional Fano plot will show a collision strength increasing linearly with the logarithm of the energy (nonrelativistically) if the inelastic transition has nonzero dipole moment. This important difference in the *asymptotic* form of these cross sections has been discussed many times (for example, Refs. 1–4, 8) although confusion still arises on occasion in the literature.

F. Domain of validity of the asymptotic cross section

The (first) Born approximation may be justified when the colliding atoms glance each other so that

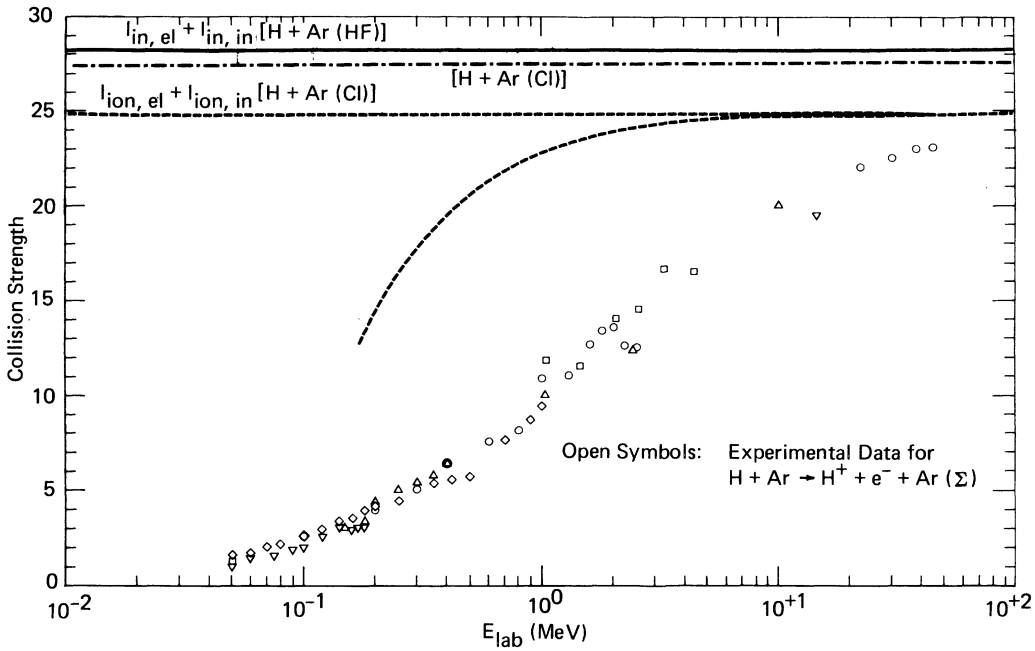

FIG. 12. Comparison of theoretical asymptotic collision strength with experiment for H+ Ar. Open symbols are $(8\pi a_0^2\alpha^2/\beta^2)^{-1}\sigma_{0,1}$ where $\sigma_{0,1}$ are the experimental cross sections for electron loss from atomic H colliding with Ar. Data are shown only for energies above that corresponding to the maximum experimental cross sections (~50 keV), and are taken from: ▽ 0.05–0.18 MeV, Solov'ev *et al.* (Ref. 25); 14.6 MeV, Smythe and Toevs (Ref. 27); △ 0.15–0.4 MeV, Puckett *et al.* (Ref. 28); 1.0 and 2.4 MeV, Welsh *et al.* (Ref. 29); 10 MeV, Berkner *et al.* (Ref. 30); □ 0.05 MeV, Williams (Ref. 20); 1.05–4.4 MeV, Schryber (Ref. 38); ◇ 0.05–0.2 MeV, Steir and Barnett (Ref. 32); 0.25–1 MeV, Barnett and Reynolds (Ref. 33); ○ 0.1–2.5 MeV, Toburen *et al.* (Ref. 34); 22–45 MeV, Acerbi *et al.* (Ref. 23). Solid line is the theoretical result of this work for $I_{in,el}+I_{in,in}$, which is a rigorous upper bound to the electron-loss collision strength. For comparison the theoretical electron-loss collision strength $I_{ion,el}+I_{ion,in}$ from Ref. 4 is given by the dashed line, and the dashed curve shows that collision strength including next-order (low-energy) corrections.

the influence of the collision on atomic electrons may be regarded as small perturbations. If the colliding atoms come so close that their electronic clouds overlap each other, there must be appreciable effects that cannot be adequately treated by the Born approximation. Thus, the differential cross section $d\sigma_{mn}$ given by Eq. (4) may be suitable at small K values (which imply unappreciable deflection of the atomic motion), but will be inappropriate at large K values (which imply appreciable deflection and thus penetration of atomic cores). This distinction in terms of the momentum transfer K is more crucial than the frequently invoked distinction in terms of the collision speed v *alone*. For inelastic collisions of a structureless charged particle with an atom or molecule, the importance of the momentum transfer as a criterion for the validity of the Born approximation is well known[7]. For example, the Lassettre-Skerbele-Dillon limit theorem[41] tells us that the Born-approximation differential cross section is correct at any v in the limit $K \to 0$ (which, however, is not rigorously realizable for any inelastic collision). Indeed, the basic argument applies just as well to collisions between atoms or molecules. For illustration, we may quote another work of Huo,[42] who successfully treated transfer of electronic excitation upon *thermal collisions* between molecules by use of the Born-approximation formula. In the process Huo discussed, the colliding partners interact predominantly at large distances by dipole-dipole forces, and therefore the justification of her treatment is especially obvious.

For collisions between ground-state atoms, the *differential cross section* $d\sigma_{mn}$ of Eq. (4) is not easily justifiable by a wave-mechanical argument, unless v greatly exceeds the mean speed v_e of the atomic electrons pertinent to the collision process. Nevertheless, a far less restrictive condition for the validity of the Born-approximation expression for the *integrated cross section* σ_{mn} was given long ago by Mott[43] and Frame,[44] who showed the equivalence of the Born integrated cross section with the result of the semiclassical impact-parameter treatment. The Mott-Frame result is

best explained by Bethe and Jackiw,[45] and is summarized by Madison and Merzbacher,[46] as well as in Sec. 4.4 of Inokuti.[7] To recapitulate the Mott-frame result, so long as the momentum of the relative motion is much greater than the mean momentum of atomic electrons (a condition that is far less restrictive than the speed criterion $v \gg v_e$ owing to the large ratio of the atomic mass to the electron mass in general), the integrated cross section σ_{mn} is adequately given by the Born-approximation formula.

The original treatments by Mott and by Frame were developed specifically for collisions of a structureless ion with an atom. Thus, one might wonder whether the same argument might need a major revision, for collisions between particles both carrying electrons. As far as we have examined, no substantially new aspect appears in this case.

In this way, we understand that the Born-approximation expression for σ_{mn}, as well for their sums such as $\sigma_{\text{in, el}}$, $\sigma_{\text{el, in}}$, and $\sigma_{\text{in, in}}$, should be adequate so long as most of the contributions arise from small and moderate values of K. The proviso here indeed bears out for processes involving inelasticity, i.e., excitation or ionization of outermost shell electrons where $\text{Ry}/T = (v_0/v)^2 \lesssim 1$, i.e., when the laboratory collision energy is greater than about 50 keV/amu (where measured cross sections often show a maximum).

The asymptotic collision strength, i.e., the constant value of the product $T\sigma$, is attained at a much higher collision energy, i.e., $\text{Ry}/T \ll 1$. Inspection of Figs. 10–12 gives an impression that the asymptotic collision strength applies at $\text{Ry}/T < 0.2$, or at the laboratory collision energy exceeding about 1 MeV/amu for combinations of the lightest atoms, and even at smaller Ry/T for heavier atoms.

The attainment of the constant collision strength is further delayed to still higher speeds when a heavier atom is involved, as seen in Fig. 12. One reason for the apparent overestimate of the collision strength $I_{\text{in, el}}$ and $I_{\text{ion, el}}$ for the H-Ar collision is probably the use of the elastic scattering form factor for Ar. To understand this, we recall that the cross section formula, Eq. (4), may be interpreted in terms of an impulse-approximation picture. That is to say, the colliding atoms exchange a momentum of the magnitude K, which is mostly taken up by the atomic electrons. These electrons, in turn, react to the momentum transfer in the same way as they do in a charged-particle collision, and their responses are described in Eq. (4) by the squared form factors $|F_m(K)|^2$ and $|F_n(K)|^2$ of the two atoms. Suppose that the second atom B is heavy and remains unexcited after the collision. It is well known[47] that, for elastic scattering of an electron by all but the lightest atoms, the first Born approximation is adequate only at extremely high speed—much greater than the speeds at which inelastic collisions of charged particles are well described by the Born approximation. Therefore, Eq. (4) could be easily improved through replacing $|F_{n=0}(K)|$ by $K^2 a_0 |A_0(K, v)|$, where $A_0(K, v)$ is the elastic-scattering amplitude (having the length dimension) and depends upon K and v. The amplitude $|A_0(K, v)|$ may be evaluated either from experimental data on electron scattering or from theoretical phase shifts as tabulated by Riley *et al.*,[48] for instance. This approach will result in better evaluation of the collision strengths for processes involving any of the heavier atoms that remain unexcited after collision. Indeed, basically the same idea has been used by Dewangan and Walters[49] in their simplified treatment of atom-atom collisions by use of a quasi-free-electron model.

Again because of the limited applicability of the first Born approximation to electron-atom elastic scattering, our results for $I_{\text{el, el}}$ are less reliable than those for other collision strengths.

IV. CONCLUDING COMMENTS

This work represents an initial undertaking toward the establishment of a comprehensive understanding of the systematics of fast atom-atom collisions. Because we are interested in a broad range of collision partners, we have had to restrict our attention to rather simple, yet comprehensive classifications of the possible phenomena considered. In that sense, this work is complementary to other studies that examined particular pairs of collision partners in greater detail.[1-6] By confining our calculations to the asymptotic collision strengths, we also have a convenient basis upon which to examine the systematic features and make comparisons. This simplification of our analysis, while rigorous at high speeds, leaves unanswered important questions at lower velocities regarding the applicability of the systematics discussed here. Nevertheless, we believe that many of the features displayed by our results for very fast collisions will have comparable counterparts at lower energies. For example, the *importance of shell-structure effects* on the simple scaling laws for the collision strengths should form a reasonably quantitative basis for estimating similar effects at high, but nonasymptotic energies.

Experimental data are lacking, not only at asymptotic speeds but even at moderately high speeds. A quick glance at Fig. 9 makes it obvious

that the paucity of data on atom-atom collisions makes any attempt to compare the systematics discussed in this work with experiment nearly impossible. This general lack of data is partially due to the difficulty of obtaining fast atoms (as opposed to ions). While there is certainly more data for ions, it is not clear that much information about systematics of the asymptotic collision strengths can be extracted.[19] Even for the impact ionization of atoms by ions carrying a significant number of electrons, the data are sparse.[50] Below, we offer a few suggestions for future measurements which we feel could significantly benefit our understanding of collisions at high energies.

For any experiments involving fast ions or atoms, we believe plots of the collision strength versus the logarithm of the energy (e.g., Fano-type plots such as Figs. 10–12) can shed light on the interpretation of the physics involved, because in the asymptotic region, theoretically well defined limits should be present. In support of this suggestion we recall the success such plots have achieved in clarifying the interpretation of electron-atom collisions.[7,40,51] Secondly, we note that for collisions involving either the excitation or ionization of a given atom, there is a total lack of data on the relative importance of elastic versus inelastic processes for the other collision partner. The differences between such singly inelastic and doubly inelastic collisions has been a central part of this work, of course, and has been examined to varying degrees in other studies as well.[1-6,8,49,50] We believe that experiments on doubly inelastic collisions, whose cross sections can be measured utilizing coincidence techniques, thus offer a particularly fruitful area for investigation. Simultaneous projectile-target ionization should be the simplest type of doubly inelastic cross section to measure, and we anticipate that the doubly inelastic cross sections obtained from our values of $I_{\mathrm{in,in}}$ should be close to the double ionization cross sections at high speeds. We might also reiterate from Sec. III C. that such doubly inelastic cross sections display the strongest shell-structure effects of the four classes of collisions we have considered. Finally, the absence of experimental data on high-energy elastic cross sections should be mentioned. As our calculations indicate that for most atom-atom collisions this is the dominant collision process (Fig. 7), it would seem that experimental confirmation of this would be among the stronger tests of our results. Such data may be beyond the present state-of-the-art, however, since the experiments presumably require very high-energy, and high-resolution differential cross section measurements.

Note added in proof: E. Horsdal Pedersen and L. Larsen have recently reported [J. Phys. B 12, 4099 (1979)] experiments on double ionization cross sections of the type we have suggested, for H colliding with He and Xe.

ACKNOWLEDGMENTS

Work performed by one of us (M.I.) was done under the auspices of the U. S. Department of Energy. The other of us (G.H.G.) acknowledges the generous support of the Physical Dynamics Independent Research and Development Fund.

APPENDIX: COLLISIONS BETWEEN TWO HYDROGENIC PARTICLES

When the colliding particles A and B have one electron each in the ground state, all the quantities appearing in the present treatment may be readily evaluated analytically, as first noted by Bates and Griffing,[1] who evaluated the cross sections σ_{mn} for various combinations of the final states m, n. Reference 3 comprehensively presents the collision strengths $I_{\mathrm{el,el}}$, $I_{\mathrm{el,in}}$, $I_{\mathrm{in,el}}$, and $I_{\mathrm{in,in}}$ for hydrogenic particles having any nuclear charges Z_A and Z_B.

Here we summarize in Table VI the results for collisions between two hydrogen atoms only. The doubly inelastic collisions are the most probable, the singly inelastic collisions the next most probable, and the elastic collisions the least probable. To understand how this ordering of different processes arises, let us review the

TABLE VI. Collision strength (T/Ry) $\sigma/8\pi a_0^2$ for two hydrogen atoms at large T.

Class of collision	Collision strength	Percentage
Elastic collisions	$I_{\mathrm{el,el}} = \frac{33}{280} = 0.1179$	10.10
Singly inelastic collisions resulting in excitation of either one of the two atoms	$I_{\mathrm{el,in}} + I_{\mathrm{in,el}} = \frac{29}{70} = 0.4143$	35.51
Doubly inelastic collisions	$I_{\mathrm{in,in}} = \frac{533}{840} = 0.6345$	54.39
Total	$\frac{7}{6} = 1.167$	100.00

elements of the calculations. First, consider the squared form factor for elastic collisions, i.e.,

$$w_0 \equiv |F_0(K)|^2 = (1-g)^2, \tag{A1}$$

where

$$g = [1 + \tfrac{1}{4}(Ka_0)^2]^{-2} \tag{A2}$$

for atomic hydrogen. The probability for one hydrogen atom to stay unexcited after a collision with momentum transfer K is proportional to $w_0(Ka_0)^{-4}d(Ka_0)^2$. Second, recall the incoherent scattering function

$$w_* \equiv S_{\rm inc}(K) = 1 - g^2. \tag{A3}$$

The probability for one hydrogen atom to be excited or ionized is proportional to $w_*(Ka_0)^{-4}d(Ka_0)^2$.

By subtraction of Eq. (A1) from Eq. (A3), one obtains

$$w_* - w_0 = 2g(1-g). \tag{A4}$$

The right-hand side is non-negative because $0 \leq g < 1$, according to Eq. (A2). Thus, $w^* \geq w_0$. The equality holds only when $g=0$ or $g=1$ (i.e., when $K=0$ or $K \to \infty$).

Each cross section for a collision between two hydrogen atoms is, in essence, an integral of the product of w's, according to Sec. II A. Because $w_* \geq w_0$ at all K, it is obvious that $w_*^2 \geq w_* w_0 \geq w_0^2$ at all K. Thus, one sees the reason for the ordering.

The foregoing arguments rest on the simple relation (A4) between w_0 and w_*, which holds exactly only for atomic hydrogen, and roughly for helium and lithium. For heavier neutral atoms (which we treat in the main text), w_* grows roughly as Z, while w_0 grows more like Z^2, both at intermediate values of Ka_0 that are decisive for the collision strengths. Thus we understand the significance of Fig. 7, which displays the dominant collision strength for all combinations of neutral atoms.

[1] D. R. Bates and G. W. Griffing, Proc. Phys. Soc. London Sec. A 66, 961 (1953); 67, 663 (1954); 68, 90 (1955).

[2] K. L. Bell and A. E. Kingston, in *Atomic Processes and Applications*, edited by P. G. Burke and B. L. Moiseiwitsch (North-Holland, Amsterdam, 1976), p. 493.

[3] M. Inokuti, Argonne National Laboratory Report No. ANL-76-88-I, 177, 1976 (unpublished).

[4] G. H. Gillespie, Phys. Rev. A 15, 563 (1977); 16, 943 (1977); 18, 1967 (1978).

[5] D. W. Rule, Phys. Rev. A 16, 19 (1977).

[6] V. S. Nikolaev, V. S. Senashenko, V. A. Sidorovich, and V. Yu. Shafer, Zh. Tekh. Fiz. 48, 1399 (1978) [Sov. Phys.-Tech. Phys. 23, 789 (1978)].

[7] M. Inokuti, Rev. Mod. Phys. 43, 297 (1971); M. Inokuti, Y. Itikawa, and J. E. Turner, Rev. Mod. Phys. 50, 23 (1978).

[8] G. H. Gillespie, Y.-K. Kim, and K. T. Cheng, Phys. Rev. A 17, 1284 (1978).

[9] A. R. P. Rau and U. Fano, Phys. Rev. 162, 68 (1967).

[10] M. Inokuti, Y.-K. Kim, and R. L. Platzman, Phys. Rev. 164, 55 (1967).

[11] J. H. Hubbell, Wm. J. Viegele, E. A. Briggs, R. T. Brown, D. T. Cromer, and R. J. Howerton, J. Phys. Chem. Ref. Data 4, 471 (1975); 6, 615 (1977).

[12] R. T. Brown, Phys. Rev. A 1, 1342 (1970); 2, 614 (1970); 5, 2141 (1972); 10, 438 (1974); J. Chem. Phys. 55, 353 (1971).

[13] D. T. Cromer and J. B. Mann, Acta Crystallogr. A 24, Part 2, 321 (1968); J. Chem. Phys. 47, 1892 (1967); D. T. Cromer, J. Chem. Phys. 50, 4857 (1969).

[14] K. Tanaka and F. Sasaki, Int. J. Quantum Chem. 5, 157 (1971).

[15] M. Naon, M. Cornille, and Y.-K. Kim, J. Phys. B 8, 864 (1975).

[16] M. Inokuti, R. P. Saxon, and J. L. Dehmer, Int. J. Radiat. Phys. Chem. 7, 109 (1975).

[17] C. F. Fischer, *The Hartree-Fock Method for Atoms: A Numerical Approach* (Wiley, New York, 1977), pp. 28–34; for He see also C. L. Pekeris, Phys. Rev. 115, 1216 (1959).

[18] These mean reduced collision strengths ($\vartheta_{\rm el,el}$, $\vartheta_{\rm el,in}$, and $\vartheta_{\rm in,in}$) were calculated by a least-squares fit to Eqs. (36)–(38) using the data in Tables II and III. The high-Z collision strengths are weighted most heavily in this procedure; the largest deviations from the fit thus occur at low Z.

[19] R. C. Dehmel, H. K. Chau, and H. H. Fleischmann, At. Data 5, 231 (1973).

[20] H. Tawara and A. Russek, Rev. Mod. Phys. 45, 178 (1973).

[21] E. H. Pedersen and P. Hvelplund, J. Phys. B 6, 1277 (1973).

[22] E. H. Pedersen and P. Hvelplund, J. Phys. B 7, 132 (1974).

[23] E. Acerbi, C. Birattari, B. Candoni, M. Castiglioni, D. Cutrupi, and C. Succi, Lett. Nuovo Cimento 10, 598 (1974).

[24] R. C. Webber and C. Hojvat, IEEE Trans. Nucl. Sci. NS-26, 4012 (1979).

[25] E. S. Solov'ev, R. N. Il'in, V. A. Oparin, and N. V. Fedorenko, Zh. Eksp. Teor. Fiz. 42, 659 (1962) [Sov. Phys.—JETP 15, 459 (1962)].

[26] G. I. Dimov and V. G. Dudnikov, Zh. Tekh. Fiz. 36, 1239 (1966) [Sov. Phys.-Tech. Phys. 11, 919 (1967)].

[27] R. Smythe and J. W. Toevs, Phys. Rev. 139, A15 (1965).

[28] L. J. Puckett, G. O. Taylor, and D. W. Martin, Phys. Rev. 178, 271 (1969).

[29] L. M. Welsh, K. H. Berkner, S. N. Kaplan, and R. V. Pyle, Phys. Rev. 158, 85 (1967).

[30] K. H. Berkner, S. N. Kaplan, and R. V. Pyle, Phys. Rev. 134, A1461 (1964).

[31] J. F. Williams, Phys. Rev. 153, 116 (1967); 157, 97 (1967).

[32] P. M. Stier and C. F. Barnett, Phys. Rev. 103, 896 (1956).

[33]C. F. Barnett and H. K. Reynolds, Phys. Rev. 109, 355 (1958).
[34]L. H. Toburen, M. Y. Nakai, and R. A. Langley, Phys. Rev. 171, 114 (1968).
[35]S. K. Allison, Phys. Rev. 110, 670 (1958).
[36]L. I. Pivovar, V. M. Tubaev, and M. T. Novikov, Zh. Eksp. Teor. Fiz. 41, 26 (1961) [Sov. Phys.—JETP 14, 20 (1962)].
[37]H. B. Gilbody, K. F. Dunn, R. Browning, and C. J. Latimer, J. Phys. B 3, 1105 (1970).
[38]U. Schryber, Helv. Phys. Acta 40, 1023 (1967).
[39]For further discussion of this point for H+ Ar see H. Levy, II, Phys. Rev. 185, 7 (1969); H. R. J. Walters, J. Phys. B 8, L54 (1975); also Ref. 49.
[40]U. Fano, Annu. Rev. Nucl. Sci. 13, 1 (1963).
[41]E. N. Lassettre, A. Skerbele, and M. A. Dillon, J. Chem. Phys. 50, 1829 (1969).
[42]W. M. Huo, J. Chem. Phys. 66, 3572 (1977).
[43]N. F. Mott, Proc. Cambridge Philos. Soc. 27, 553 (1931).
[44]J. W. Frame, Proc. Cambridge Philos. Soc. 27, 511 (1931).
[45]H. A. Bethe and R. W. Jackiw, *Intermediate Quantum Mechanics*, 2nd ed. (Benjamin, New York, 1968), Chap. 19, p. 321.
[46]D. H. Madison and E. Merzbacher, in *Atomic Inner-Shell Processes*: Vol. 1, Ionization and Transition Probabilities, edited by B. Craseman (Academic, New York, 1975), p. 1.
[47]R. A. Bonham and M. Fink, *High-Energy Electron Scattering* (Van Nostrand, New York, 1974).
[48]M. E. Riley, C. J. MacCallum, and F. Biggs, At. Data Nucl. Data Tables 15, 443 (1975).
[49]D. P. Dewangan and H. R. J. Walters, J. Phys. B 11, 3983 (1978).
[50]For example, see G. H. Gillespie, Phys. Lett. A72, 329 (1979); or L. H. Toburen and W. E. Wilson, Phys. Rev. A 19, 2214 (1979), as well as references cited therein.
[51]J. Kistemaker, in *Electronic and Atomic Collisions*, edited by N. Oda and K. Takayanagi (North-Holland, Amsterdam, 1980), p. 3; M. Inokuti, *ibid.*, p. 31, as well as references cited therein.